HHS Public Access

Author manuscript

Cell Rep. Author manuscript; available in PMC 2019 August 27.

Published in final edited form as:

Cell Rep. 2019 August 13; 28(7): 1758–1772.e4. doi:10.1016/j.celrep.2019.07.034.

Context-Dependent Role for T-bet in T Follicular Helper Differentiation and Germinal Center Function following Viral Infection

Amania A. Sheikh[1,2], **Lucy Cooper**[3,4], **Meiqi Feng**[1,2], **Fernando Souza-Fonseca-Guimaraes**[1,2], **Fanny Lafouresse**[1,5], **Brigette C. Duckworth**[1,2], **Nicholas D. Huntington**[1,2,3,4], **James J. Moon**[6], **Marc Pellegrini**[2,7], **Stephen L. Nutt**[1,2], **Gabrielle T. Belz**[1,2], **Kim L. Good-Jacobson**[3,4], **Joanna R. Groom**[1,2,8,*]

[1]Division of Immunology, Walter and Eliza Hall Institute of Medical Research, Parkville, VIC 3052, Australia

[2]Department of Medical Biology, University of Melbourne, Parkville, VIC 3010, Australia

[3]Department of Biochemistry and Molecular Biology, Monash University, Clayton, VIC 3800, Australia

[4]Biomedicine Discovery Institute, Monash University, Clayton, VIC 3800, Australia

[5]Centre de Recherches en Cancerologie de Toulouse, INSERM U1037, Equipe labellisee Ligue Nationale contre le cancer, University de Toulouse III-Paul Sabatier, Toulouse, France

[6]Center for Immunology and Inflammatory Diseases, and Division of Pulmonary and Critical Care Medicine, Massachusetts General Hospital, and Harvard Medical School, Charlestown, MA 02129, USA

[7]Division of Infection and Immunity, Walter and Eliza Hall Institute of Medical Research, Parkville, VIC 3052, Australia

[8]Lead Contact

SUMMARY

Following infection, inflammatory cues upregulate core transcriptional programs to establish pathogen-specific protection. In viral infections, T follicular helper (TFH) cells express the prototypical T helper 1 transcription factor T-bet. Several studies have demonstrated essential but conflicting roles for T-bet in TFH biology. Understanding the basis of this controversy is crucial, as modulation of T-bet expression instructs TFH differentiation and ultimately protective antibody

*Correspondence: groom@wehi.edu.au.

AUTHOR CONTRIBUTIONS

J.R.G. designed the research. A.A.S. performed the majority of the experiments. L.C., M.F., and F.S.-F.-G. performed additional experiments. K.L.G.-J., G.T.B., S.L.N., M.P., J.J.M., F.L., B.C.D., and N.D.H. provided technical assistance, reagents, and intellectual input. J.R.G. and A.A.S. analyzed the experiments and wrote the manuscript.

DECLARATION OF INTERESTS

The authors declare no conflicts of interest.

SUPPLEMENTAL INFORMATION

Supplemental Information can be found online at https://doi.org/10.1016/j.celrep.2019.07.034.

responses. Comparing influenza and LCMV viral infections, we demonstrate that the role of T-bet is contingent on the environmental setting of TFH differentiation, IL-2 signaling, and T cell competition. Furthermore, we demonstrate that T-bet expression by either TFH or GC B cells independently drives antibody isotype class switching. Specifically, T cell-specific loss of T-bet promotes IgG1, whereas B cell-specific loss of T-bet inhibits IgG2a/c switching. Combined, this work highlights that the context-dependent induction of T-bet instructs the development of protective, neutralizing antibodies following viral infection or vaccination.

In Brief

Shiekh et al. show that, in influenza and LCMV infections, the role of the transcription factor T-bet in TFH differentiation is contingent on environmental cues, IL-2 signaling, and T cell competition. Cell-specific T-bet expression independently drives antibody isotype class switching. Therefore T-bet instructs immune protection in a context-dependent manner.

Graphical Abstract

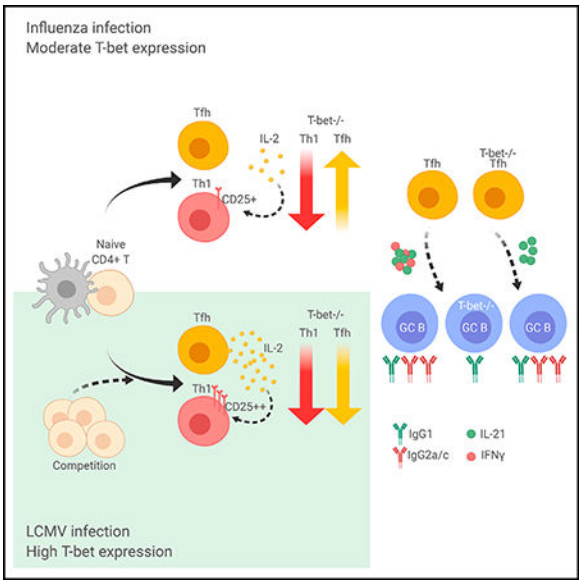

INTRODUCTION

Germinal centers (GCs) are specialized microstructures formed during immune responses and are the cornerstone of protective adaptive immunity. Within GCs, T follicular helper (TFH) cells provide B cells with signals essential for B cell differentiation into isotype-switched antibody-secreting cells. Multiple cytokines and cellular interactions coordinate the expression of a core group of transcription factors that regulate both GC T and B cell differentiation, identity, and function (Good-Jacobson and Groom, 2018). Principally, during both TFH and GC B cell differentiation, Bcl6 upregulation occurs with the reciprocal downregulation of its agonist, B lymphocyte-induced protein-1 (Blimp1) (Crotty et al., 2010; Johnston et al., 2009). In TFH cells, Bcl6 is a transcriptional repressor that acts via multiple mechanisms to functionally activate TFH signature genes and inhibit the different

effector T helper (TH) fates (Hatzi et al., 2015; Nurieva et al., 2009; Yu et al., 2009). Despite Bcl6-mediated repression of alternative TH fates, TFH differentiation occurs in parallel with other TH cells. Following viral infection, several prototypical TH1 cell molecules are simultaneously expressed by TFH cells. Notably, this includes co-expression and binding of Bcl6 and the TH1 lineage-specifying transcription factor T-bet (Johnston et al., 2009; Lu et al., 2011; Lüthje et al., 2012; Nakayamada et al., 2011; Oestreich et al., 2011). This interplay is functionally relevant, as T-bet physically recruits Bcl6 to suppress transcription of target genes and blocks the Bcl6 DNA-binding domain, thus establishing appropriate gene expression in TH1 cells (Oestreich et al., 2011, 2012). Similarly, Bcl6 and T-bet can also be co-expressed in B cells following viral infection (Kallies and Good-Jacobson, 2017; Piovesan et al., 2017; Stone et al., 2019). Therefore, the balance in the ratios of different lineage-defining transcription factors may independently alter GC cell function. How extrinsic factors such as distinct infections instruct transcription factor expression and balance is not understood, however, this critically determines cellular differentiation outcomes and ultimately immunological protection.

T-bet is an essential regulator of cellular differentiation and function within multiple lineages. T-bet is the lineage-defining transcription factor for TH1 cells, and it is also highly expressed in $CD8^+$ CTLs, as well as some B and innate lymphoid cell subsets (Kallies and Good-Jacobson, 2017). Following viral infection, T cells exhibit graded induction of T-bet expression, which corresponds with their functional capacity. In $CD8^+$ T cells, T-bet functions as a molecular switch between effector and memory differentiation (Intlekofer et al., 2007; Joshi et al., 2007). High expression of T-bet induces and cooperates with Zeb2 to enact a unique transcriptional program that forces effector cell differentiation (Dominguez et al., 2015). In TFH cell differentiation, the role of T-bet is less clear and is an area of active investigation. As T-bet-Bcl6 complexes can inhibit Bcl6 DNA binding, it has been proposed that expression of T-bet during $CD4^+$ T cell activation intrinsically tips the balance of differentiation in favor of TH1 cells (Oestreich et al., 2012). This hypothesis is supported by initial studies in T-bet-deficient animals showing an increased accumulation of TFH cells and reciprocal loss of TH1 cells *in vitro* and following *Toxoplasma gondii* or *Plasmodium berghei* ANKA infections (Nakayamada et al., 2011; Ryg-Cornejo et al., 2016). In contrast, T-bet was shown to promote both TH1 and TFH cell differentiation following lymphocytic choriomeningitis virus (LCMV) infection (Wang et al., 2019; Weinstein et al., 2018). How extrinsic factors underpin these conflicting results in the role of T-bet within differentiating TFH cells and GC biology has not been established.

TFH cytokine signals play an essential role in tailoring effective GC responses (Reinhardt et al., 2009). IL-21 is the cardinal TFH-derived cytokine and along with IFNγ, IL-4, and IL-10 mediates B cell class switching and affinity maturation (Lüthje et al., 2012; Miyauchi et al., 2016; Ramiscal and Vinuesa, 2013). For example, T cell-derived IFNγ induces T-bet in B cells, leading to the upregulation of a broad anti-viral gene expression program (Barnett et al., 2016; Peng et al., 2002; Rubtsova et al., 2013). Together with IL-21, this promotes TH1-skewed antibody-producing cells and drives isotype switching of antibody to IgG2a (named IgG2c in C57BL/6 mice and hereinafter referred to as IgG2a/c) (Lüthje et al., 2012; Miyauchi et al., 2016; Peng et al., 2002; Stone et al., 2019). Switching of antibody to the IgG2a/c isotype mediates clearance of virus and protection against lethal influenza infection

(Huber et al., 2006; Miyauchi et al., 2016). In addition, the combined induction of both IgG2a/c and IgG1 is required for optimal vaccine efficacy more than neutralization alone (Huber et al., 2006). The specific external and transcriptional regulators that oversee this balance of antibody class switch following infection are not fully understood.

In this study, we determine the timing and level of expression of T-bet in GC T and B cells following influenza infection using ZsGreen_T-bet reporter mice (Zhu et al., 2012). We show that both T-bet^{+} T and B cells are found within GC structures throughout influenza infection, but T-bet levels in the GC do not reach those observed in non-GC effector T cell populations. Given the conflicting literature on the function of T-bet in humoral immunity, we sought to dissect the factors that control these divergent outcomes. We demonstrate that the role of T-bet is contingent on the environmental setting of TFH differentiation, whereby changes in pathogen and T cell competition for antigen alters the kinetics and intensity of T-bet induction, IL-2 production, and consumption and the outcome of T-bet deficiency. Furthermore, to elucidate the function of T-bet individually in GC T and B cells, we use T-bet$^{fl/fl}$ animals crossed to Cre-expressing animals for each cell type to identify the downstream outcomes of T-bet deficiency. We show that T-bet acts independently in GC T and B cells to enact isotype switching following influenza infection. This revealed that expression in TFH cells directs switching away from IgG1 isotypes, while expression within GC B cells directs switching toward IgG2a/c. Thus, our data demonstrate that T-bet expression within the different cellular compartments of GCs works together to mediate efficient isotype switching that will effectively neutralize virus.

RESULTS

T-bet-Expressing Cells Are Located within GC Structures following Influenza Infection

To characterize the expression of T-bet following influenza infection, we made use of the ZsGreen_T-bet reporter mouse, which faithfully reports the expression of *Tbx21* transcript (Zhu et al., 2012). *Tbx21* transcription has previously been shown to be repressed by Bcl6, but despite this, we found considerable reporter expression within the GC structures of the draining mediastinal lymph node (dLN) at day 8 (d8) following intranasal infection with influenza A HKx31 (H3N2) (Figure 1A). This expression was seen early in infection, with T-bet^{+}GL7^{+} cells detected at d4, prior to established GC structures. T-bet expression was observed following the establishment of GCs d8 and d14 post-infection (p.i). T-bet-expressing cells were present in both the CD35^{+} FDC-marked light zone (LZ; GL7^{+}IgD^{-}CD35^{+}) and to a lesser extent within the dark zone (DZ; GL7^{+}IgD^{-}CD35^{-}) (Figure 1A, bottom panels). Furthermore, co-staining with CD4 and B220 showed that both GC T and B cells were positive for *Tbx21* expression (Figures 1B and 1C). We next identified in more detail the T-bet-expressing subsets within GCs using flow cytometry. For this we tracked the upregulation and expression of T-bet^{+} cells in dLN during influenza infection. Polyclonal T cell responses were tracked using the gating strategy of Marshall et al. (2011) to identify dLN TH1 cells (CD44^{+}PSGL-1^{+}Ly6c^{+}) and TFH cells (CD44^{+}PSGL-1^{-}Ly6c^{-}PD-1^{+}CXCR5^{+}) (Marshall et al., 2011). As expected, TH1 cells rapidly upregulated high levels of *Tbx21,* which peaked at d8-d14 of infection (Figures 1D–1F). T-bet expression within the TFH compartment followed a similar kinetic to that of TH1 cells, peaking

between d8-d10 of infection. However, TFH cells showed 1–2 logs lower ZsGreen_T-bet reporter expression than the peak MFI of TH1 cells (Figure 1D). This lower expression of T-bet within the TFH compartment is reminiscent of the graded T-bet expression found within the $CD8^+$ T cell compartment, which determines cell fate decisions between effector and memory differentiation (Intlekofer et al., 2007; Joshi et al., 2007). We next identified the kinetics of T-bet induction in GC^+ B cells ($B220^+IgD^-CD95^+$ $CD38^-$) and plasma cells ($B220^{lo}CD138^+$) in dLNs. Within both B cell populations, *Tbx21* transcripts peaked at d8 following infection (Figures 1G–1I). Similar to TFH cells, T-bet^+ B cells expressed a lower level of ZsGreen_T-bet reporter expression than seen in TH1 cells (Figure 1G). Potentially, the lower expression of *Tbx21* within TFH, GC B, and plasma cells may indicate a common mechanism of transcriptional repression that is not present in TH1 and $CD8^+$ T cells (Figures 1D and 1G and data not shown).

T Cell-Specific T-bet Expression Promotes the Accumulation of TH1 Cells with Reciprocal Loss of TFH Cells

As we had observed T-bet expression in GC T and B cells at the peak of the influenza inflammatory response, we next dissected the role of T-bet during TH1 and TFH differentiation *in vivo* at d8 following infection. Initially, we used intact T-bet-deficient (*Tbx21*$^{-/-}$) animals to confirm previous results that indicated *Tbx21* deficiency promotes TFH cell differentiation *in vivo* (Figure S1) (Nakayamada et al., 2011; Ryg-Cornejo et al., 2016). TFH differentiation *in vivo* is a dynamic, multi-step process that relies on interactions with both dendritic cells and B cells (Groom, 2015; Qi, 2016). To determine whether these differences were T cell intrinsic, we investigated mice lacking T-bet in all T cells (*Tbx21*$^{fl/fl}$xCD4Cre, *Tbx21*ΔT) following influenza infection. *Tbx21*ΔT and CD4Cre controls were infected, and polyclonal T cell responses were assessed (Figures 2A–2D). This analysis confirmed that T cell-specific *Tbx21* deficiency does indeed promote the accumulation of TFH cells with a reciprocal loss of TH1 cell differentiation. Furthermore, using MHCII I-A^b-restricted tetramers, we identified $CD4^+$ T cells specific for the immunodominant epitope $NP_{311–325}$ of influenza A virus. We found no differences in the frequency or numbers of NP_{311} $tetramer^+$ cells following infection between CD4Cre controls and *Tbx21*ΔT animals (Figures 2E and 2F). Similar to that observed in the polyclonal population, within the NP_{311} $tetramer^+$ cells, TH1 showed a reduced accumulation, while non-TH1 frequency and TFH numbers were increased (Figures 2G–2J). Combined, these results demonstrate that T-bet acts as a molecular switch that determines $CD4^+$ T cell differentiation between TFH and TH1 effector cells.

The Role of T-bet in $CD4^+$ T Cell Differentiation Is Context and Competition Dependent

In contrast to our data, STAT4-dependent induction of T-bet in $CD4^+$ T cells has been shown to promote the differentiation of both TH1 and TFH cell differentiation following LCMV infection, and in the absence of *Tbx21,* both TH1 and TFH differentiation is limited (Wang et al., 2019; Weinstein et al., 2018). We were intrigued as to how these divergent results may arise and sought to replicate this experimental model. Antigen-specific Smarta TCR Tg cells (STg; specific for the LCMV immunodominant epitope $GP_{66–77}$) and *Tbx21*ΔT STg cells were transferred into wild-type hosts prior to LCMV (Armstrong) intravenous infection. Splenic STg TH1 and TFH cells were determined *in vivo* at d8 following infection (Figures

3A–3D). Following transfer of cells, the frequency of TH1 cells was significantly decreased in *Tbx21*ΔT STg cells, with a reciprocal increase in the number of non-TH1 cells (STg $^{+}$CD44^{+}PSGL-1^{-}Ly6c^{-}) (Figures 3A and 3B). Despite the accumulation of activated, non-TH1 cells, these cells failed to upregulate TFH markers PD-1 and CXCR5, resulting in a deficiency of both TH1 and TFH cells and a complete deficiency in effector CD4^{+} T cell differentiation. These results are consistent with recent work (Weinstein et al., 2018) but contrast with our findings in intact *Tbx21*ΔT following influenza infection (Figure 2). Thus, T-bet mediates divergent CD4^{+} T cell differentiation outcomes, which are contingent on the infectious and experimental setting.

Fate decisions between TH1 and TFH can be determined by multiple factors, including antigen affinity and signal strength, in addition to T cell competition for both antigen and environmental cytokines (DiToro et al., 2018; Qi, 2016; Ramiscal and Vinuesa, 2013). These environmental cues lead to the upregulation and balance of multiple transcription factors that regulate CD4^{+} T cell differentiation (Good-Jacobson and Groom, 2018; Oestreich et al., 2012). It therefore seemed likely that changes in these conditions during an infection could alter the outcome of T-bet deficiency during TFH cell differentiation. To gain insight into the factors that determine the role of T-bet during T cell activation and differentiation, we altered key experimental parameters to understand how viral infection and T cell competition affect TFH differentiation following viral infection. Given that *Tbx21*ΔT STg cells were transferred into a competitive environment with wild-type cells, we reasoned that this competition may significantly alter the outcome of T-bet deficiency following LCMV infection (Figure 3C). To address this question, *Tbx21*ΔT animals were infected with LCMV, and splenic CD4^{+} T cells specific for the MHCII I-A^{b}-restricted immunodominant epitope GP$_{66–77}$ of LCMV were assessed at d8 following infection. In these conditions, without competing wild-type T cells, the role of T-bet again resembled what we had observed for influenza infection in both *Tbx21*$^{-/-}$ and *Tbx21*ΔT mice, in which TH1 cells failed to accumulate with a reciprocal increase in the frequency of TFH cells (Figures 3G–3J). We next altered the T cell competition environment of *Tbx21*ΔT mice in influenza infection using a 50:50 BM chimera approach. In this setting, GP$_{66}$ tetramer^{+} *Tbx21*ΔT TH1 cell frequency was reduced together and was accompanied by diminished accumulation of non-TH1 cells and limited TFH differentiation (Figure S2). Combined, these results suggest that when *Tbx21*ΔT CD4^{+} T cells are required to compete with wild-type counterparts, the accumulation of effector cells is reduced for both TH1 and TFH cells.

Context-Specific Induction of T-bet Alters T Cell Proliferation, Activation Marker Expression, and Transcription Factor Ratios

To investigate the context-specific basis for the role of T-bet during TFH differentiation, we analyzed in detail the viral infectious settings with the most divergent outcomes: influenza infection in intact animals and LCMV infection with STg transfer (Figure 4). Comparing the ZsGreen_T-bet reporter in these infections showed marked differences in T-bet induction at d4 and d8 during each immune response. Early in LCMV infection, both TFH and TH1 strongly induced T-bet compared with T cells in influenza infection (Figures 4A and 4B). At d8 the frequency of T-bet^{+} in influenza TH1 cells resembled that of LCMV TFH cells, while T-bet was expressed to a lesser extent in influenza TFH cells. We next investigated how the

loss of T-bet expression in these settings influenced proliferation and differentiation readouts during TFH and TH1 differentiation. Using Ki67 as a marker for proliferating cells (Miller et al., 2018), we showed that LCMV induced a higher rate of proliferation at d4 compared with influenza infection (Figures 4C and 4D). Ki67 MFI showed the context-specific role of T-bet whereby at d4 p.i., Ki67 intensity was reduced with T-bet deficiency and increased in influenza. At d8 of infection, the tetramer$^+$ TFH cells in influenza infection showed increased Ki67 expression over that of STg cells in LCMV, but this was not altered further by T-bet deficiency (Figure 4D). We found the kinetics in expression of key regulators of TFH cell differentiation and function was altered in a viral-dependent fashion (Figures 4E–4J). PD-1, Bcl6, and CXCR5 were all more highly expressed in LCMV than influenza d4 of infection, but this was reversed at d8 in TFH cells for PD-1 and Bcl6 (Figures 4E and 4F; Figure S3). Furthermore, at d4 of LCMV and d8 of both LCMV and influenza, T-bet was required for the induction of CXCR3, which may help position cells within GC structures (Figures 4G and 4H; Good-Jacobson and Groom, 2018; Groom, 2015; Kallies and Good-Jacobson, 2017; Shi et al., 2018). Similarly, CD25 also showed context-dependent expression that was regulated by T-bet deficiency at d4 p.i. (Figures 4I and 4J). Combined, this work demonstrates that unique viral infections and T cell competition finely tune TFH differentiation in the context of divergent T-bet induction.

Divergent Induction of T-bet during Viral Infection Alters the Balance of IL-2 Production and Signaling

The different induction of T-bet in two Th1-biased infection models likely reflects unique cytokine milieu between infections. Multiple inflammatory cytokines, including IL-2,TGFβ, IL-7, IL-6, and type I IFNs, alter the balance between TH1 and TFH cells during infection (Ballesteros-Tato et al., 2012; Choi et al., 2011; DiToro et al., 2018; Eto et al., 2011; Harker et al., 2011; Marshall et al., 2015; McDonald et al., 2016; Oestreich et al., 2011; Ray et al., 2014). As we observed that CD25 MFI was altered in a viral- and T-bet-dependent manner (Figures 4I and 4J), we next investigated the role IL-2 production and consumption play in TFH differentiation between influenza and LCMV infections. The prevailing paradigm for IL-2 CD4$^+$T cell fate decisions dictates that CD25 marks IL-2 consumers that become TH1 cells, while early producers of IL-2 become TFH cells (Ballesteros-Tato et al., 2012; DiToro et al., 2018; Oestreich et al., 2011; Pepper et al., 2011). Fitting this hypothesis, at d4 of infection, CD25 expression was segregated from CXCR5 expression in LCMV infection (Figure 5A). However, the separation of cell fates by CD25 or IL-2 was less well defined in influenza infection (Figures 5A–5C), with low expression of CD25, and the low-affinity IL-2 receptor CD122 was also minimally expressed (Figures S4A and S4B). To demonstrate that the differential expression of CD25 between infections and genotypes was functionally relevant, we determined STAT5 phosphorylation following a brief IL-2 stimulation. Phosphorylated STAT5 (pSTAT5) correlated with the expression of CD25, while no pSTAT5 was detected without IL-2 (Figures 5D and 5E; Figures S4C and S4D). This expression was further dependent on T-bet, whereby CD25$^+$pSTAT5$^+$ frequency in T-bet-deficient T cells was increased in influenza but decreased in LCMV. Furthermore, we investigated whether IL-2 production serves as a marker of TFH differentiation. Similar to described work, at d4, IL-2$^+$ cells were found predominately in the CXCR5$^+$ STg cells following LCMV infection

(Figures 5F and 5G). However, in influenza IL-2 production did not indicate CXCR5 cells at this time, suggesting early demarcation of T cell fate is less clear in this infection model.

T Cell-Intrinsic T-bet Deficiency Influences TFH Cytokine Production but Leaves GC B Cell Differentiation Intact

The identification of an experimental model in which *Tbx21* deficiency resulted in the expansion of TFH cells allowed the opportunity to dissect the functional role of T-bet within individual cellular compartments of GCs in intact animals. We first investigated the production of TFH cytokine in *Tbx21*ΔT and control animals following influenza infection by crossing CD4Cre and *Tbx21*ΔT to an IL-21^{GFP} reporter (Lüthje et al., 2012). As T-bet directly controls IFNγ production, we predictably showed a significant decrease in IFNγ production by *Tbx21*ΔT TFH cells following PMA and ionomycin stimulation (Figures 6A and 6B). Interestingly, this drop in IFNγ production appeared to be more significant in influenza compared with published data in LCMV infection (Weinstein et al., 2018) and is in line with fate-mapping data indicating that previous or current T-bet expression is essential for TFH IFNγ production (Fang et al., 2018). Similar to effects on T cell differentiation, the role of T-bet in production of IL-21 may also differ depending on experimental model, with some studies reporting an increase in IL-21 with T-bet-deficiency whereas others show no difference (Lüthje et al., 2012; Nakayamada et al., 2011; Schmitt et al., 2016; Weinstein et al., 2018). Following influenza infection, we did not see an overall change in IL-21 production in *Tbx21*ΔT TFH cells (Figures 6A and 6B). However, combined with the drop in IFNγ, this resulted in a net loss of double-positive IL-21^{+}IFNγ^{+} cells, which may indicate altered functionality of IL-21-expressing TFH population with GCs (Figure 6C). Furthermore, although IL-21 has previously been shown to be produced by CXCR3^{+} TH1 cells, this could not be detected in our experimental system in either control or *Tbx21*ΔT mice (data not shown) (Miyauchi et al., 2016).

We next sought to determine the overall affect that T cell-intrinsic loss of T-bet had on GC B cell responses. We examined GC B cell differentiation by flow cytometry at d8 following influenza infection in *Tbx21*ΔT and CD4Cre mice. We detected an increase in the frequency and total number of GC B cells within dLN, in line with the increased expansion of TFH cells in *Tbx21*ΔT animals (Figures 6D and 6E). However, we did not see any overt effect on the proportion of cells in the LZ (CXCR4^{-}CD86^{+}) or DZ (CXCR4^{+}CD86^{-}) compartments (Figure 6F; Figure S5A). Furthermore, we quantified the number and size of GC structures (GL7^{+}IgD^{-}) in dLNs. We found no difference in the overall size and number of GC structures, suggesting that the expansion of GC B cell numbers was not sufficient to be detected by confocal microscopy (Figure 6G; Figure S5B). Therefore, T cell-intrinsic T-bet deficiency does not result in an overt GC B cell phenotype.

B Cell-Intrinsic T-bet Deficiency Does Not Alter GC Structure

As we and others had observed T-bet expression in GC B cells (Figures 1G–1I), we next investigated the reciprocal question, as to the B cell-intrinsic role of T-bet within GC reactions (Kallies and Good-Jacobson, 2017; Piovesan et al., 2017; Stone et al., 2019). For this we examined *Tbx21*$^{fl/fl}$xCD23Cre (*Tbx21*ΔB) animals at d8 following influenza infection (Piovesan et al., 2017). We found no statistical differences in GC B cell numbers,

LZ/DZ accumulation, or GC number and structure between *Tbx21*ΔB and CD23Cre control animals (Figures 6H–6L; Figures S5C and S5D). Therefore, B cell-intrinsic deficiency of T-bet does not result in any overt GC phenotype as examined either by flow cytometry or histologically.

T-bet Acts Independently within TFH and GC B Cells to Influence Isotype Class Switching

Antigen-specific B cells interpret T cell cytokine signals to determine the class switch isoform of high-affinity antibodies. We therefore sought to determine the independent roles of T-bet in T and B cells for antibody class switching. Initially, we identified the level of surface IgG1 and IgG2a/c present on GC B cells at d8 following influenza infection. Comparing complete *Tbx21*$^{-/-}$ animals with controls, we showed not only the expected defect in IgG2a/c but a reciprocal increase in IgG1 (Figures 7A and 7B). GC B cells from *Tbx21*ΔT mice showed no deficiency in IgG2a/c but an increase in IgG1 GC B cell surface staining (Figures 7C and 7D). In contrast, *Tbx21*ΔB GC B cells showed reduced IgG2a/c surface staining as previously described, but no change in IgG1 (Figures 7E and 7F) (Peng et al., 2002; Piovesan et al., 2017). CD138^{+} plasma cells also showed a similar switching bias to GC B cells in each genotype examined (data not shown). We next investigated how differences in isotype switching affect the serum concentration IgG isotypes over the course of influenza infection. Consistent with our IgG isotype surface staining, *Tbx21*$^{-/-}$ animals showed increased IgG1 and decreased IgG2a/c levels over the course of infection (Figures 7G and 7H). Again, T cell-intrinsic T-bet deficiency resulted in increased serum IgG1 (Figures 7I and 7J), while B cell-intrinsic T-bet deficiency resulted in increased serum IgG2a/c (Figures 7K and 7L). Together these cell intrinsic phenotypes observed in individual T and B cell *Tbx21*-deficient animals summed to recapitulate the isotype switching phenotype seen in *Tbx21*$^{-/-}$ animals. Thus, T-bet acts independently in TFH and GC B cells to tailor isotype switching following influenza infection.

DISCUSSION

In this study, we identify T-bet as a molecular switch that determines CD4^{+} T cell differentiation outcomes following different viral infections. In comparison with TH1 cells, TFH and B cells express lower levels of *Tbx21* throughout the immune response to influenza infection. This graded expression between populations is reminiscent of that seen in CD8^{+} cells with different effector and memory potential (Dominguez et al., 2015; Joshi et al., 2007). T-bet has been shown to be differentially induced following infections with distinct cytokine skewing, for example, TH1 and TH2-skewed infection models (Wang et al., 2019; Zhu et al., 2012). Here, we describe that T-bet expression is graded in cell subsets even between viral models that are thought to evoke similar cytokine skewing. It is interesting to speculate if an overarching rheostat for T-bet expression exists in TFH cells to determine these context-specific differentiation outcomes. We have previously shown that c-Myb can act in this manner in GC B cells to instruct the levels of T-bet depending on the environmental context (Piovesan et al., 2017).

IL-2 signaling plays a central role in the determination of TH1 and TFH bifurcation (Ballesteros-Tato et al., 2012; Choi et al., 2011; DiToro et al., 2018), whereby IL-2 restricts

Bcl6 expression and promotes the differentiation of TH1 cells (Oestreich et al., 2012). TGFβ also acts upstream of CD25 expression to inhibit IL-2 signaling (Marshall et al., 2015). Similarly, IL-7 and type I IFNs repress the TFH program (McDonald et al., 2016; Ray et al., 2014), while IL-6 promotes TFH expansion and functional GC reactions (Eto et al., 2011; Harker et al., 2011). We show distinct IL-2 expression between our model infections, but other inflammatory cytokines may also drive altered T-bet induction in these systems. IFNγ plays a critical role in promoting T-bet in TH1 cells, while IL-12 drives T-bet expression in $CD8^+$ T cells (Joshi et al., 2007; Kallies and Good-Jacobson, 2017). Our data suggest that the distinct infection routes (intranasal and intravenous) and level of viral tropism (low and high, respectively) for influenza and LCMV contribute to the differential cytokine production and inflammatory cell recruitment present at the time of T cell priming. Together these viral factors, along with antigen affinity and viral load are intertwined with environmental cytokines to determine the upregulation and overall balance of T-bet and Bcl6 within TFH and GC B cells (DiToro et al., 2018; Fahey et al., 2011; Harker et al., 2011; Snook et al., 2018). That these distinctions alter the role of T-bet during TFH differentiation shifts the dogma of viewing all viral infections in a canonical manner to one in which individual inflammatory and viral factors should be considered when assigning roles for transcriptional regulation of T cell differentiation.

Here we show that T-bet is differentially induced between two important and widely used TH1-biased infection models. Specifically, strong expression in TFH andTH1 precursors in LCMV and TH1 precursors in influenza infection reflects the essential role for T-bet in differentiation of these cell fates. Conversely the lower expression seen in TFH precursors in influenza correlates with the accumulation of these cells in the absence of T-bet. These divergent infections models also uniquely influence the T cell precursor ratios of IL-2 consumers and producers, and this is further augmented with T-bet deficiency. Although T cell differentiation during LCMV infection adheres to the current paradigm that IL-2 production and signaling determine the fate of $CD4^+$ cells in viral infection, this segregation is less clear for influenza, in which T-bet expression and cell fate decisions appear to occur later in infection. This delay potentially allows influenza-specific TFH precursors to pass a survival checkpoint that is not permitted when T-bet is highly induced.

Our findings clarify previous contradictory findings for the role of T-bet in TH1/TFH bifurcation by indicating that transcription factor thresholds are different depending on the environmental context of T-bet and Bcl6 upregulation. Several previous studies have reported that T-bet intrinsically tips the balance of $CD4^+$ T cell differentiation in favor of TH1 cell differentiation in multiple infectious settings (Marshall et al., 2011; Nakayamada et al., 2011; Oestreich et al., 2012; Ryg-Cornejo et al., 2016). Our results in intact animals are also in line with human TFH cells, where T-bet does not inhibit the differentiation of $CXCR5^+$ TFH-like cells (Schmitt et al., 2016). In contrast, we show, along with Weinstein et al. (2018), that the presence of competing T cells, which may influence the availability of the proliferative and differentiation cytokines or antigen, is a key factor in determining the role of T-bet in TH1/TFH fate outcomes (Weinstein et al., 2018). Combined, this work highlights distinct induction of T-bet in specific experimental systems and emphasizes the importance of understanding T-bet modulation when considering vaccination strategies when TFH IFNγ production and/or specific IgG class switching is a major goal.

Within GCs, TFH cells and B cells upregulate a core group of transcription factors (Good-Jacobson and Groom, 2018). Our data suggest that despite shared expression, T-bet acts independently in each cellular compartment to influence class switching following viral infection. Although switching of antibody to the IgG2a/c isotype mediates clearance of virus and protection against lethal influenza infection, IgG1 is required for optimal vaccine efficacy (Huber et al., 2006; Miyauchi et al., 2016). Thus, the overall distribution of antibody isotype is critical for immune protection. T-bet plays a central role in this balance, acting both intrinsically in GC B cells to promote IgG2a/c and indirectly, presumably through TFH cytokine production, to lower IgG1 production. Combined, these results identify T-bet as a context-dependent link between extrinsic inflammatory signals and intrinsic cellular differentiation programs and highlights the importance of understanding the context of T-bet induction for the development of protective, neutralizing antibodies following viral infection and vaccination.

STAR★METHODS

LEAD CONTACT AND MATERIALS AVAILABILITY

Further information and requests for resources and reagents should be directed to and will be fulfilled by Lead Contact, Joanna Groom (groom@wehi.edu.au).

EXPERIMENTAL MODEL AND SUBJECT DETAILS

Mice and BM chimeras—Mice were maintained on a C57BL/6 background in specific-pathogen-free conditions. ZsGreen_T-bet reporter (Zhu et al., 2012), T-bet$^{fl/fl}$ (Wang et al., 2012), T-bet$^{fl/fl}$ CD23Cre (*Tbx21*ΔB) (Piovesan et al., 2017), *Tbx21*$^{-/-}$ (Finotto et al., 2002), Smarta TCR transgenic (STg) (Oxenius et al., 1998) mice have been previously described. T-bet$^{fl/fl}$ were crossed with CD4Cre to generate T-bet$^{fl/fl}$ CD4Cre (*Tbx21*ΔT). *Tbx21*ΔT and CD4Cre were bred with IL21^{GFP} (Lüthje et al., 2012) reporter mice. *Tbx21*ΔT mice were crossed to GFP and STg to generate GFP Stg and *Tbx21*ΔT STg respectively. Both male and female mice at 6–10 weeks of age were used in this study. Mixed chimeras were generated by lethally irradiated Ly5.1xC57BL/6 mice (two doses of 0.55 Cy) and reconstitution with *Tbx21*ΔT and Ly5.1 bone marrow in a 1:1 ratio. Mice were left for 8 weeks before infection. All experiments were performed in accordance with the Walter and Eliza Hall Institute animal ethics committee.

METHOD DETAILS

Viral infections and Adoptive transfer—Mice were inoculated intranasally with 1×10^4 PFU influenza virus strain HKx31 (H3N2) or intravenously with 2×10^5or3×10^3 PFU LCMV Armstrong for d4 and d8 experiments respectively. For adoptive transfer, STg CD4$^+$T cell were isolated by naive CD4$^+$T cell negative selection kit and 2.0×10^5 (for d4) or 2.5×10^4 (for d8) naive GFP STg or Tbx21ΔT STg cells were transferred independently to non-irradiated naive recipient mice via intravenous injection. Mice were infected with LCMV the day following cell transfer.

Tetramer staining and Flow Cytometry—Tissues were mechanically dissociated to single cell suspensions and enriched for CD4$^+$ T cells following an incubation with cocktail

of antibodies (listed in Key Resource Table) to deplete non-$CD4^+$ T cell lineages. Antibody-bound cells were removed by magnetic bead depletion using BioMag Goat anti-Rat IgG beads. Enriched $CD4^+$T cells were stained with $NP_{311–325}$:1-A^b or $GP_{66–77}$:1-A^b, conjugated with streptavidin-PE tetramer for 1h at room temperature (Moon et al., 2011). Cells were stained using indicated antibodies (Key Resource Table) and intracellular proteins were detected using Foxp3 staining kit according to manufacturer's protocol. Cytokine intracellular staining experiment was performed as previously described (Lüthje et al., 2012). For pSTAT5 detection, T cells were stimulated in round bottom plates in the presence of 100U/mL murine recombinant IL-2 (DNAX Research Institute) for 25 min at 37 degrees. Intracellular staining of pSTAT5 fixation and permeabilization with Lyse/Fix and Perm III buffers (BD Biosciences) as previously described (Viel et al., 2016). Cytometry data was acquired using a LSR Fortessa x-20 (BD Biosciences).

Immunofluorescence staining—Lymph nodes were fixed in 4% paraformaldehyde and immersed in 30% sucrose before being embedded in OCT compound (Tissue-Tek). Tissues were cut via microtome (Leica) into 12–20 μm sections and mounted on Superfrost Plus slides. Sections were stained as described previously (Rankin et al., 2013) using described antibodies (Key Resource Table). Images were acquired using a LSM780 confocal microscope (Carl Zeiss MicroImaging). The acquisition software was Zen Black 2012 and images were quantified with ImageJ (NIH).

Enzyme-linked immunosorbent assay (ELISA)—Antibodies for detection of total serum are listed (Key Resource Table). 96-well flat-bottom ELISA plates (Sarstedt) were coated with 75 μL per well of respective unlabeled coating antibody (diluted in PBS) 4°C overnight. Plates were blocked with PBS 1% BSA at room temperature for 1h. Plates were washed three times with PBS Tween20 and dH2O. Samples and standards were added to the wells and blank wells were included (PBS 1%BSA). Plates were incubated for 2–4h at 37°C before being washed three times. Secondary antibody, HRP (horseradish peroxidase) diluted in PBS 1%BSA was added and incubated at 37°C for 2h. The plates were then washed five times and 100 μL of OPD (o-phenylenediamine dihydrochloride) substrate solution (ThermoFisher Scientific) was added and plates incubated room temperature in the dark for 10–30 minutes to develop. OD values were read at 405nm using a plate reader (BMG Labtech) and the data was evaluated using MARS (BMG Labtech).

QUANTIFICATION AND STATISTICAL ANALYSIS

Flow cytometry was analyzed using Flowjo (Treestar) and statistical significance was determined using the paired (for chimeric experiments) or unpaired (two-tailed) Student's t test. For ELISA, differences between the groups were analyzed using the MannWhitney non-parametric two-tailed test with a 95% confidence. All experimental data is presented as mean ± standard error of the mean (SEM) with statistical analysis performed using Prism 7 (GraphPad Software).

Supplementary Material

Refer to Web version on PubMed Central for supplementary material.

ACKNOWLEDGMENTS

We thank members of the Groom lab for technical assistance and Leisa-Rebecca Watson, who performed initial experiments. This work was supported by National Health and Medical Research Council (NHMRC) project grants to J.R.G. and K.L.G.-J. (GNT1137989 and GNT1057707) and to M.P. (GNT1006592, GNT1045549, and GNT1065626) and by NIH grants to J.J.M. (R01 AI107020 and R21 AI124143). A.A.S. and B.C.D. are supported by a University of Melbourne research scholarship. J.R.G. is supported by an Australian Research Council Future Fellowship (FT130100708). K.L.G.-J. is supported by an NHMRC Career Development Fellowship (1108066). G.T.B. and S.L.N. are supported by an NHMRC Senior Principal Research Fellowship. K.L.G.-J. and M.P. are supported by Bellberry-Viertel and Sylvia & Charles Viertel Senior Medical Research Fellowships. L.C. received a Biomedicine Discovery Institute Scholarship from Monash University. F.L. is supported by a Walter and Eliza Hall Centenary Fellowship sponsored by CSL. This work was made possible through Victorian State Government Operational Infrastructure Support and the Australian Government NHMRC Independent Research Institute Infrastructure Support Scheme (IRIISS).

REFERENCES

Ballesteros-Tato A, León B, Graf BA, Moquin A, Adams PS, Lund FE, and Randall TD (2012). Interleukin-2 inhibits germinal center formation by limiting T follicular helper cell differentiation. Immunity 36, 847–856. [PubMed: 22464171]

Barnett BE, Staupe RP, Odorizzi PM, Palko O, Tomov VT, Mahan AE, Gunn B, Chen D, Paley MA, Alter G, et al. (2016). Cutting edge: B cell-intrinsic T-bet expression is required to control chronic viral infection. J. Immunol 797, 1017–1022.

Choi YS, Kageyama R, Eto D, Escobar TC, Johnston RJ, Monticelli L, Lao C, and Crotty S (2011). ICOS receptor instructs T follicular helper cell versus effector cell differentiation via induction of the transcriptional repressor Bcl6. Immunity 34, 932–946. [PubMed: 21636296]

Crotty S, Johnston RJ, and Schoenberger SP (2010). Effectors and memories: Bcl-6 and Blimp-1 in T and B lymphocyte differentiation. Nat. Immunol 11, 114–120. [PubMed: 20084069]

DiToro D, Winstead CJ, Pham D, Witte S, Andargachew R, Singer JR, Wilson CG, Zindl CL, Luther RJ, Silberger DJ, et al. (2018). Differential IL-2 expression defines developmental fates of follicular versus nonfollicular helper T cells. Science 361, eaao2933. [PubMed: 30213884]

Dominguez CX, Amezquita RA, Guan T, Marshall HD, Joshi NS, Kleinstein SH, and Kaech SM (2015). The transcription factors ZEB2 and T-bet cooperate to program cytotoxic T cell terminal differentiation in response to LCMV viral infection. J. Exp. Med 212, 2041–2056. [PubMed: 26503446]

Eto D, Lao C, DiToro D, Barnett B, Escobar TC, Kageyama R, Yusuf I, and Crotty S (2011). IL-21 and IL-6 are critical for different aspects of B cell immunity and redundantly induce optimal follicular helper CD4 T cell (Tfh) differentiation. PLoS ONE 6, e17739. [PubMed: 21423809]

Fahey LM, Wilson EB, Elsaesser H, Fistonich CD, McGavern DB, and Brooks DG (2011). Viral persistence redirects CD4 T cell differentiation toward T follicular helper cells. J. Exp. Med 208, 987–999. [PubMed: 21536743]

Fang D, Cui K, Mao K, Hu G, Li R, Zheng M, Riteau N, Reiner SL, Sher A, Zhao K, and Zhu J (2018). Transient T-bet expression functionally specifies a distinct T follicular helper subset. J. Exp. Med 215, 2705–2714. [PubMed: 30232200]

Finotto S, Neurath MF, Glickman JN, Qin S, Lehr HA, Green FH, Ackerman K, Haley K, Galle PR, Szabo SJ, et al. (2002). Development of spontaneous airway changes consistent with human asthma in mice lacking T-bet. Science 295, 336–338. [PubMed: 11786643]

Good-Jacobson KL, and Groom JR (2018). Tailoring immune responses toward autoimmunity: transcriptional regulators that drive the creation and collusion of autoreactive lymphocytes. Front. Immunol 9, 482. [PubMed: 29568300]

Groom JR (2015). Moving to the suburbs: T-cell positioning within lymph nodes during activation and memory. Immunol. Cell Biol 93, 330–336. [PubMed: 25753266]

Harker JA, Lewis GM, Mack L, and Zuniga EI (2011). Late interleukin-6 escalates T follicular helper cell responses and controls a chronic viral infection. Science 334, 825–829. [PubMed: 21960530]

Hatzi K, Nance JP, Kroenke MA, Bothwell M, Haddad EK, Melnick A, and Crotty S (2015). BCL6 orchestrates Tfh cell differentiation via multiple distinct mechanisms. J. Exp. Med 212, 539–553. [PubMed: 25824819]

Huber VC, McKeon RM, Brackin MN, Miller LA, Keating R, Brown SA, Makarova N, Perez DR, Macdonald GH, and McCullers JA (2006). Distinct contributions of vaccine-induced immunoglobulin G1 (IgG1) and IgG2a antibodies to protective immunity against influenza. Clin. Vaccine Immunol 13, 981–990. [PubMed: 16960108]

Intlekofer AM, Takemoto N, Kao C, Banerjee A, Schambach F, Northrop JK, Shen H, Wherry EJ, and Reiner SL (2007). Requirement for T-bet in the aberrant differentiation of unhelped memory $CD8^+$ T cells. J. Exp. Med 204, 2015–2021. [PubMed: 17698591]

Johnston RJ, Poholek AC, DiToro D, Yusuf I, Eto D, Barnett B, Dent AL, Craft J, and Crotty S (2009). Bcl6 and Blimp-1 are reciprocal and antagonistic regulators of T follicular helper cell differentiation. Science 325, 1006–1010. [PubMed: 19608860]

Joshi NS, Cui W, Chandele A, Lee HK, Urso DR, Hagman J, Gapin L, and Kaech SM (2007). Inflammation directs memory precursor and shortlived effector CD8(+) T cell fates via the graded expression of T-bet transcription factor. Immunity 27, 281–295. [PubMed: 17723218]

Kallies A, and Good-Jacobson KL (2017). Transcription factor T-bet orchestrates lineage development and function in the immune system. Trends Immunol. 38, 287–297. [PubMed: 28279590]

Lu KT, Kanno Y, Cannons JL, Handon R, Bible P, Elkahloun AG, Anderson SM, Wei L, Sun H, O'Shea JJ, and Schwartzberg PL (2011). Functional and epigenetic studies reveal multistep differentiation and plasticity of in vitro-generated and in vivo-derived follicular T helper cells. Immunity 35, 622–632. [PubMed: 22018472]

Lüthje K, Kallies A, Shimohakamada Y, Belz GT, Light A, Tarlinton DM, and Nutt SL (2012). The development and fate of follicular helper T cells defined by an IL-21 reporter mouse. Nat. Immunol 13, 491–498. [PubMed: 22466669]

Marshall HD, Chandele A, Jung YW, Meng H, Poholek AC, Parish IA, Rutishauser R, Cui W, Kleinstein SH, Craft J, and Kaech SM (2011). Differential expression of Ly6C and T-bet distinguish effector and memory Th1 CD4(+) cell properties during viral infection. Immunity 35, 633–646. [PubMed: 22018471]

Marshall HD, Ray JP, Laidlaw BJ, Zhang N, Gawande D, Staron MM, Craft J, and Kaech SM (2015). The transforming growth factor beta signaling pathway is critical for the formation of CD4 T follicular helper cells and isotype-switched antibody responses in the lung mucosa. eLife 4, e04851. [PubMed: 25569154]

McDonald PW, Read KA, Baker CE, Anderson AE, Powell MD, Ballesteros-Tato A, and Oestreich KJ (2016). IL-7 signalling represses Bcl-6 and the TFH gene program. Nat. Commun 7, 10285. [PubMed: 26743592]

Miller I, Min M, Yang C, Tian C, Gookin S, Carter D, and Spencer SL (2018). Ki67 is a graded rather than a binary marker of proliferation versus quiescence. Cell Rep. 24, 1105–1112.e5. [PubMed: 30067968]

Miyauchi K, Sugimoto-Ishige A, Harada Y, Adachi Y, Usami Y, Kaji T, Inoue K, Hasegawa H, Watanabe T, Hijikata A, et al. (2016). Protective neutralizing influenza antibody response in the absence of T follicular helper cells. Nat. Immunol 17, 1447–1458. [PubMed: 27798619]

Moon JJ, Dash P, Oguin TH 3rd, McClaren JL, Chu HH, Thomas PG, and Jenkins MK (2011). Quantitative impact of thymic selection on Foxp3+ and Foxp3− subsets of self-peptide/MHC class II-specific CD4+ T cells. Proc. Natl. Acad. Sci. USA 108, 14602–14607. [PubMed: 21873213]

Nakayamada S, Kanno Y, Takahashi H, Jankovic D, Lu KT, Johnson TA, Sun HW, Vahedi G, Hakim O, Handon R, et al. (2011). Early Th1 cell differentiation is marked by a Tfh cell-like transition. Immunity 35,919–931. [PubMed: 22195747]

Nurieva RI, Chung Y, Martinez GJ, Yang XO, Tanaka S, Matskevitch TD, Wang YH, and Dong C (2009). Bcl6 mediates the development of T follicular helper cells. Science 325, 1001–1005. [PubMed: 19628815]

Oestreich KJ, Huang AC, and Weinmann AS (2011). The lineage-defining factors T-bet and Bcl-6 collaborate to regulate Th1 gene expression patterns. J. Exp. Med 208, 1001–1013. [PubMed: 21518797]

Oestreich KJ, Mohn SE, and Weinmann AS (2012). Molecular mechanisms that control the expression and activity of Bcl-6 in TH1 cells to regulate flexibility with a TFH-like gene profile. Nat. Immunol 13, 405–411. [PubMed: 22406686]

Oxenius A, Bachmann MF, Zinkernagel RM, and Hengartner H (1998). Virus-specific MHC-class II-restricted TCR-transgenic mice: effects on humoral and cellular immune responses after viral infection. Eur. J. Immunol 28, 390–400. [PubMed: 9485218]

Peng SL, Szabo SJ, and Glimcher LH (2002). T-bet regulates IgG class switching and pathogenic autoantibody production. Proc. Natl. Acad. Sci. U S A 99, 5545–5550. [PubMed: 11960012]

Pepper M, Pagán AJ, Igyártó BZ, Taylor JJ, and Jenkins MK (2011). Opposing signals from the Bcl6 transcription factor and the interleukin-2 receptor generate T helper 1 central and effector memory cells. Immunity 35, 583–595. [PubMed: 22018468]

Piovesan D, Tempany J, Di Pietro A, Baas I, Yiannis C, O'Donnell K, Chen Y, Peperzak V, Belz GT, Mackay CR, et al. (2017). c-Myb regulates the T-bet-dependent differentiation program in B cells to coordinate antibody responses. Cell Rep. 19, 461–470. [PubMed: 28423310]

Qi H (2016). T follicular helper cells in space-time. Nat. Rev. Immunol 16, 612–625. [PubMed: 27573485]

Ramiscal RR, and Vinuesa CG (2013). T-cell subsets in the germinal center. Immunol. Rev 252, 146–155. [PubMed: 23405902]

Rankin LC, Groom JR, Chopin M, Herold MJ, Walker JA, Mielke LA, McKenzie AN, Carotta S, Nutt SL, and Belz GT (2013). The transcription factor T-bet is essential for the development of NKp46+ innate lymphocytes via the Notch pathway. Nat. Immunol 14, 389–395. [PubMed: 23455676]

Ray JP, Marshall HD, Laidlaw BJ, Staron MM, Kaech SM, and Craft J (2014). Transcription factor STAT3 and type I interferons are corepressive insulators for differentiation of follicular helper and T helper 1 cells. Immunity 40, 367–377. [PubMed: 24631156]

Reinhardt RL, Liang HE, and Locksley RM (2009). Cytokine-secreting follicular T cells shape the antibody repertoire. Nat. Immunol 10, 385–393. [PubMed: 19252490]

Rubtsova K, Rubtsov AV, van Dyk LF, Kappler JW, and Marrack P (2013). T-box transcription factor T-bet, a key player in a unique type of B-cell activation essential for effective viral clearance. Proc. Natl. Acad. Sci. U S A 110, E3216–E3224. [PubMed: 23922396]

Ryg-Cornejo V, loannidis LJ, Ly A, Chiu CY, Tellier J, Hill DL, Preston SP, Pellegrini M, Yu D, Nutt SL, et al. (2016). Severe malaria infections impair germinal center responses by inhibiting T follicular helper cell differentiation. Cell Rep. 14, 68–81. [PubMed: 26725120]

Schmitt N, Liu Y, Bentebibel SE, and Ueno H (2016). Molecular mechanisms regulating T helper 1 versus T follicular helper cell differentiation in humans. Cell Rep. 16, 1082–1095. [PubMed: 27425607]

Shi J, Hou S, Fang Q, Liu X, Liu X, and Qi H (2018). PD-1 controls follicular T helper cell positioning and function. Immunity 49, 264–274.e4. [PubMed: 30076099]

Snook JP, Kim C, and Williams MA (2018). TCR signal strength controls the differentiation of CD4+ effector and memory T cells. Sci. Immunol 3, eaas9103. [PubMed: 30030369]

Stone SL, Peel JN, Scharer CD, Risley CA, Chisolm DA, Schultz MD, Yu B, Ballesteros-Tato A, Wojciechowski W, Mousseau B, et al. (2019). T-bet transcription factor promotes antibody-secreting cell differentiation by limiting the inflammatory effects of IFN-gamma on B cells. Immunity 50, 1172–1187.e7. [PubMed: 31076359]

Viel S, Marçais A, Guimaraes FS, Loftus R, Rabilloud J, Grau M, Degouve S, Djebali S, Sanlaville A, Charrier E, et al. (2016). TGF-β inhibits the activation and functions of NK cells by repressing the mTOR pathway. Sci. Signal 9, ra19. [PubMed: 26884601]

Wang NS, McHeyzer-Williams LJ, Okitsu SL, Burris TP, Reiner SL, and McHeyzer-Williams MG (2012). Divergent transcriptional programming of class-specific B cell memory by T-bet and RORα. Nat. Immunol 13, 604–611. [PubMed: 22561605]

Wang P, Wang Y, Xie L, Xiao M, Wu J, Xu L, Bai Q, Hao Y, Huang Q, Chen X, et al. (2019). The transcription factor T-bet is required for optimal type I follicular helper T cell maintenance during acute viral infection. Front. Immunol 10, 606. [PubMed: 30984183]

Weinstein JS, Laidlaw BJ, Lu Y, Wang JK, Schulz VP, Li N, Herman EI, Kaech SM, Gallagher PG, and Craft J (2018). STAT4 and T-bet control follicular helper T cell development in viral infections. J. Exp. Med 215, 337–355. [PubMed: 29212666]

Yu D, Rao S, Tsai LM, Lee SK, He Y, Sutcliffe EL, Srivastava M, Lin-terman M, Zheng L, Simpson N, et al. (2009). The transcriptional repressor Bcl-6 directs T follicular helper cell lineage commitment. Immunity 31, 457–468. [PubMed: 19631565]

Zhu J, Jankovic D, Oler AJ, Wei G, Sharma S, Hu G, Guo L, Yagi R, Yamane H, Punkosdy G, et al. (2012). The transcription factor T-bet is induced by multiple pathways and prevents an endogenous Th2 cell program during Th1 cell responses. Immunity 37, 660–673. [PubMed: 23041064]

Highlights

- In influenza infection, T-bet represses TFH cells to promote TH1 differentiation
- T-bet is required for differentiation of both TFH and TH1 cells following LCMV
- Distinct IL-2 signaling, T cell competition, and T-bet threshold between infections
- T cell- and B cell-specific T-bet together balance IgG1 and IgG2a/c isotype switching

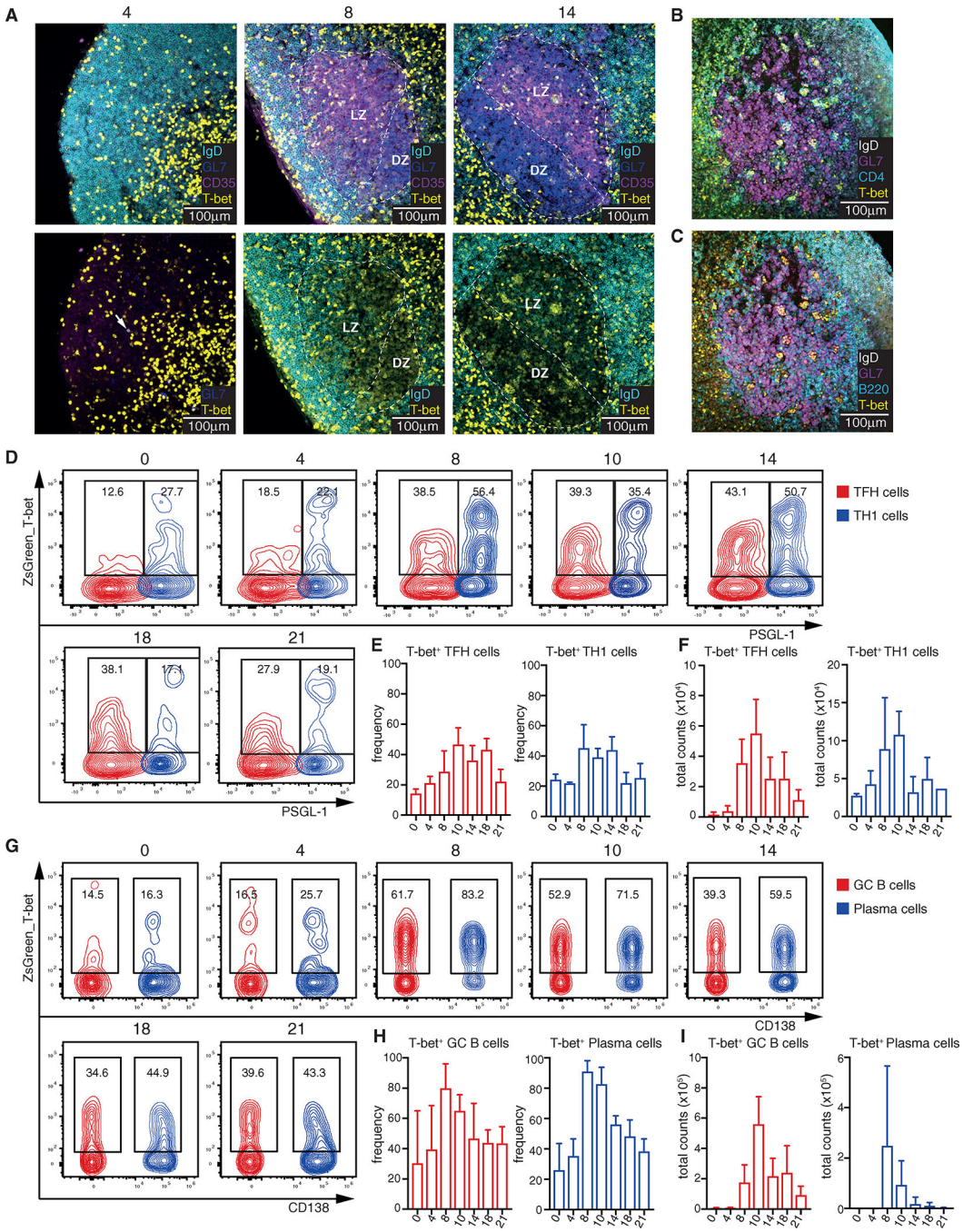

Figure 1. T and B GC Cells Express T-bet Following Influenza Infection

ZsGreen_T-bet reporter mice were infected with influenza and dLNs analyzed. (A–C) Representative confocal micrograph at indicated days p.i. T-bet$^+$ cells (yellow) in GC LZ (IgD$^-$GL7$^+$CD35$^+$) and DZ (IgD$^-$GL7$^+$CD35$^+$). Arrow indicates T-bet$^+$GL7$^+$ cell at d4 p.i. Dashed lines mark GC regions, bottom panels show T-bet$^+$ cells without GC markers (A). Day 8 p.i. T-bet$^+$ GC co-stained with CD4 (cyan) (B) and co-stained with B220 (cyan) (C).

(D) Representative flow cytometry plots showing frequency of T-bet^{+} TFH (red, CD44^{+}PSGL-1^{-} Ly6c^{-} PD-1^{+} CXCR5^{+}) and T-bet^{+} TH1 (blue, CD44^{+} PSGL-1^{+}Ly6c^{+}) at indicated days p.i.

(E and F) Frequency (E) and total numbers (F) of T-bet^{+} TFH and TH1 cells.

(G) Flow cytometry plots showing frequency of T-bet^{+} GC B cells (red, B220^{+}IgD^{-}CD95^{+}CD38^{-}) and plasma cells (blue, B220^{lo} CD138^{+}).

(H and I) Frequency (H) and total numbers (I) of T-bet^{+} GC B and plasma cells.

In (E), (F), (H), and (I), data are pooled from three independent experiments. Data are mean ± SEM.

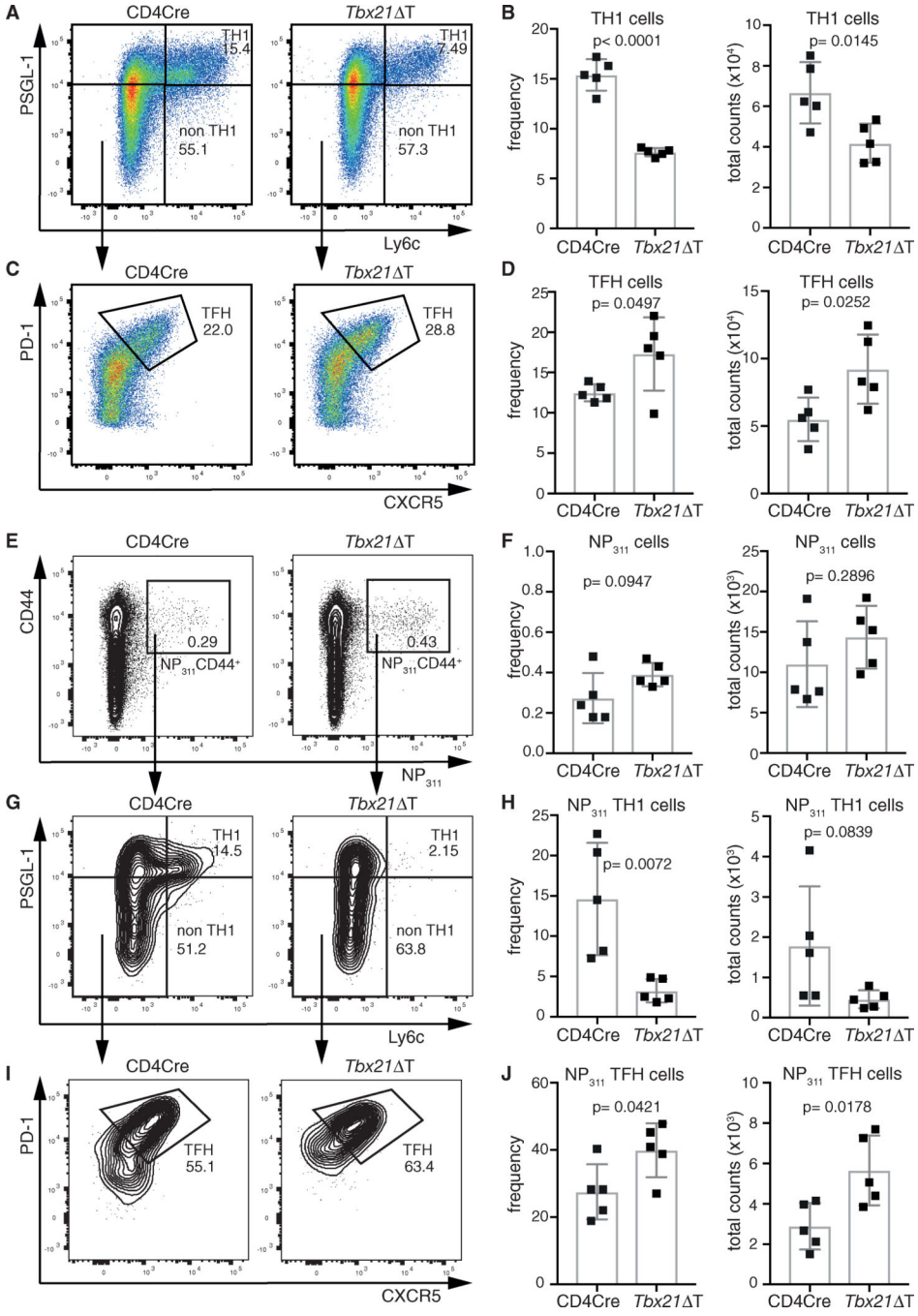

Figure 2. T Cell-Specific *Tbx21* Deficiency Promotes TFH Differentiation following Influenza Infection

CD4cre and *Tbx21*ΔT mice were infected with influenza, and dLN $CD4^+CD44^+$ polyclonal and antigen-specific cells were analyzed at d8 p.i.

(A–D) Representative flow cytometry plots of polyclonal $CD4^+CD44^+$ (A and C) with frequency and total number (B and D) of natural repertoire of TH1 ($CD44^+PSGL\text{-}1^+Ly6c^+$) (A and B) and TFH ($CD44^+PSGL\text{-}1^-Ly6c^-PD1^+CXCR5^+$) (C and D).

(E and F) Plots (E) and frequency and total number (F) of NP_{311} $CD4^+$ T cells.

(G–J) Plots (G and I) and frequency and total number (H and J) of TH1 ($NP_{311}^{+}CD44^{+}PSGL\text{-}1^{+}Ly6c^{+}$) (G and H) and TFH ($NP_{311}^{+}$ $PSGL\text{-}1^{-}Ly6c^{-}PD\text{-}1^{+}CXCR5^{+}$) (I and J).

Data are representative of three independent experiments, n = 3–5 mice/group. Data are mean ± SEM.

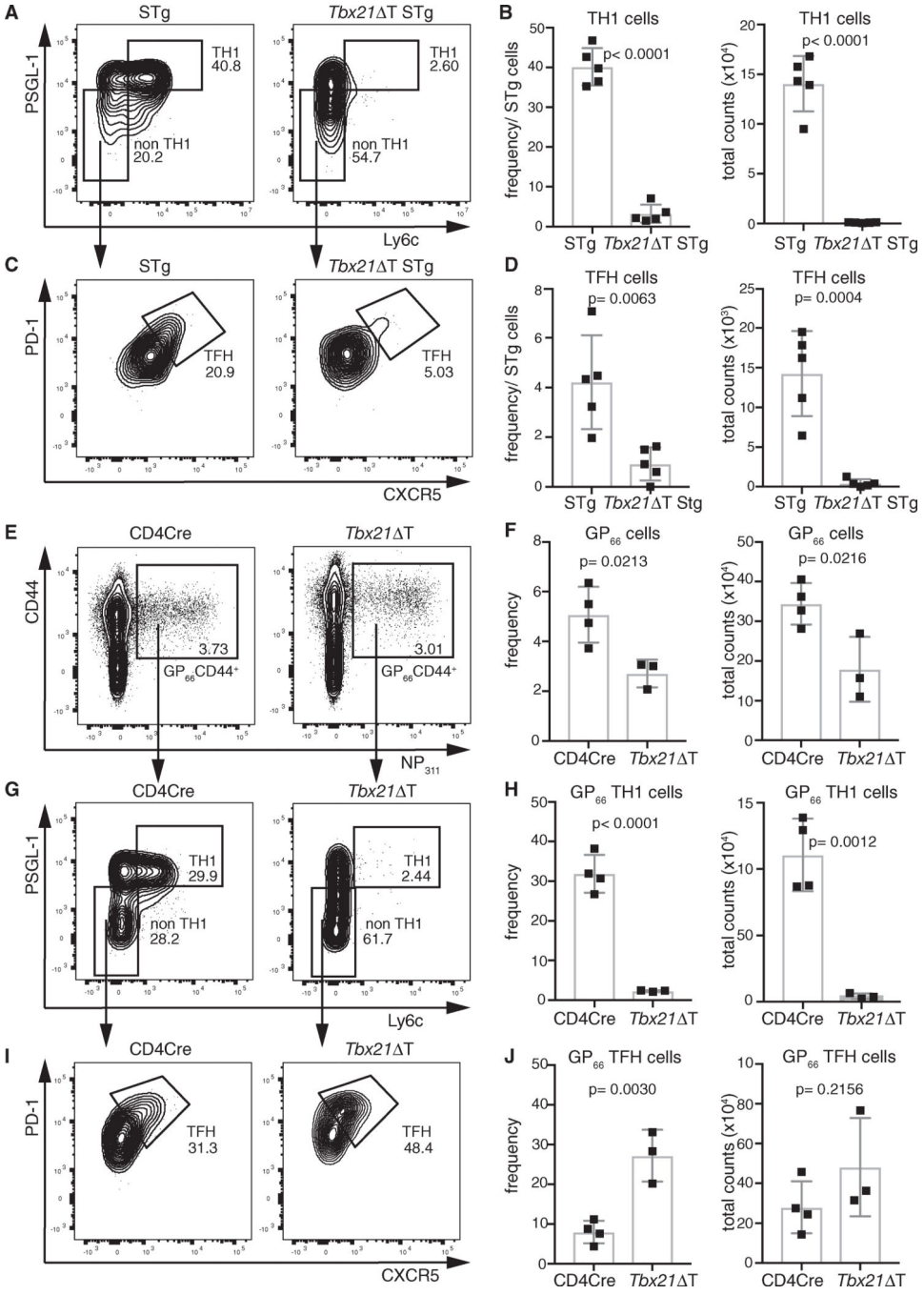

Figure 3. T-bet Regulates TFH Differentiation in a Context-Dependent Manner following LCMV Infection

(A–D) STg and *Tbx21*ΔT STg were transferred into Ly5.1xLy5.2 F1 mice subsequently infected with LCMV, and splenic STg cells were analyzed at d8 p.i. Representative flow cytometry plots (A and C) and frequency and total number (B and D) of TH1 ($CD44^+PSGL\text{-}1^+Ly6c^+$) (A and B) and TFH ($CD44^+PSGL\text{-}1^-Ly6c^-PD\text{-}1^+CXCR5^+$) (C and D) in indicated mice.

(E–J) CD4cre and *Tbx21*ΔT mice were infected with LCMV, and splenic $CD4^+CD44^+$ antigen-specific cells were analyzed at d8 p.i. Plots (E) and frequency and total number (F)

of GP_{66} $CD4^+$ T cells. Plots (G and I) and frequency and number (H and J) of TH1 ($GP_{66}^+CD44^+PSGL\text{-}1^+Ly6c^+$) (G and H) and TFH ($GP_{66}^+CD44^+PSGL\text{-}1^-Ly6c^-PD\text{-}1^+CXCR5^+$) (I and J).

Data are representative of three independent experiments, n = 3–5 mice/group. Data are mean ± SEM.

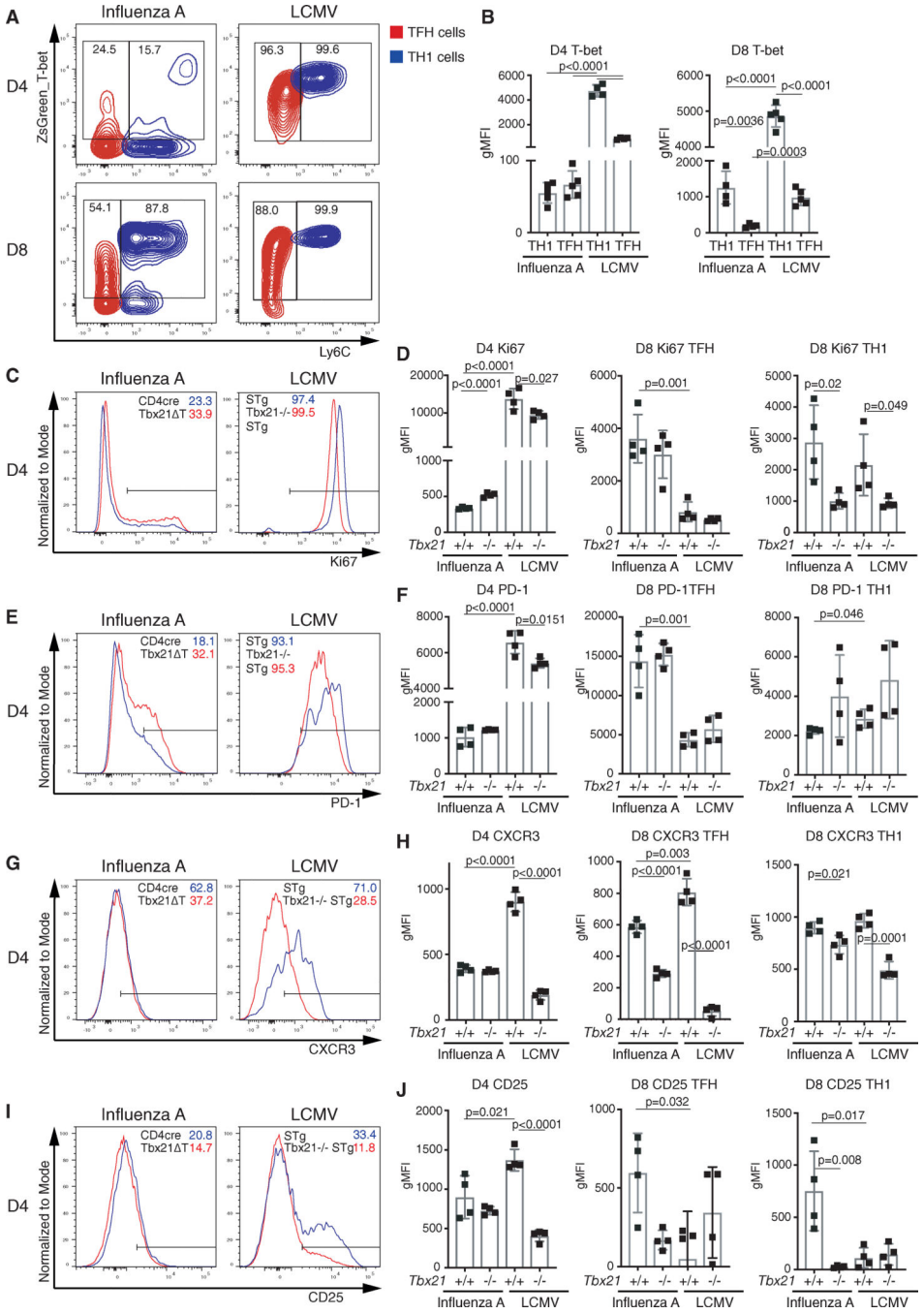

Figure 4. Viral-Specific Induction of T-bet Alters Proliferation, Activation, and Transcription Factor Ratios during T Cell Differentiation

(A and B) ZsGreen_T-bet reporter mice were infected with influenza or naive ZsGreen_T-bet STg cells were transferred prior to LCMV infection. Draining lymph nodes (influenza) and splenocytes (LCMV) were harvested at d4 and d8 p.i. Representative flow cytometry plots (A) and MFI of activated (d4) and NP_{311} (d8) and STg TFH (red) and TH1 (blue) (B) in indicated infection models.

(C–J) CD4cre and *Tbx21*ΔT mice were infected with influenza or naive STg or $Tbx21^{-/-}$ STg cells were transferred prior to LCMV infection and analyzed at d4 and d8 p.i. Activated

T cells ($CD4^+CD44^+$) and $tetramer^+$ ($NP311^+$ were assessed respectively for d4 and d8 p.i. influenza infection. STg cells were assessed for LCMV time points. Viral specific cells were assessed for Ki67 MFI (C and D), PD-1 MFI (E and F), CXCR3 MFI (G and H), and CD25 MFI (I and J). Representative histograms show frequency in positive gate.

Data are representative of two or three independent experiments, n = 3–5 mice/group. Data are mean ± SEM.

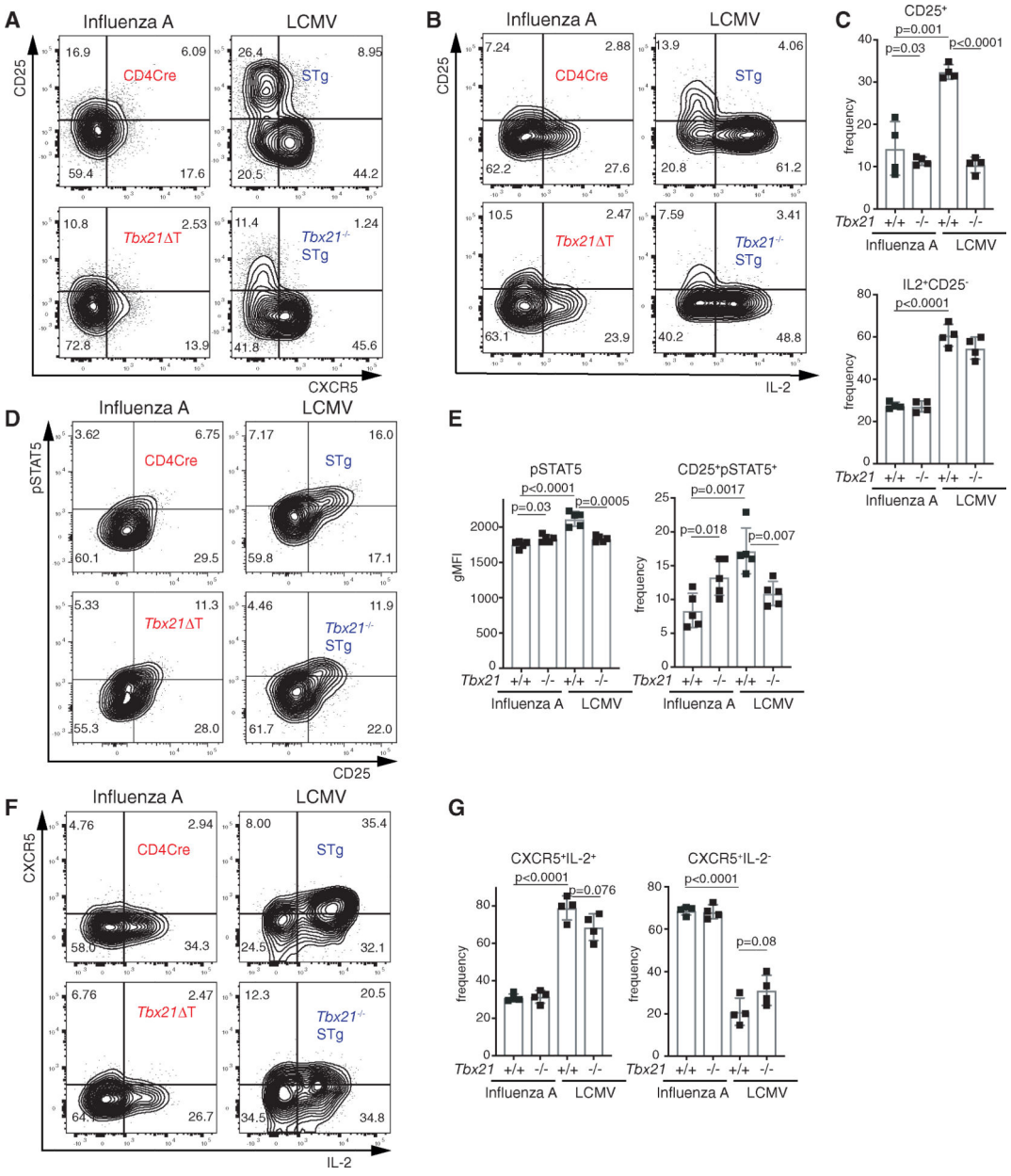

Figure 5. Differential Production and Consumption of IL-2 in Influenza and LCMV Infection Models

CD4cre and *Tbx21*ΔT mice were infected with influenza or naive STg or Tbx21$^{-/-}$ STg cells were transferred prior to LCMV infection and analyzed at d4 p.i. Activated T cells (CD4^{+}CD44^{+}) and STg cells were assessed for influenza and LCMV infections, respectively.

(A–C) Representative flow cytometry plots (A and B) and frequency (C) of CD25^{+} and IL-2^{+} cells in indicated models. Note that re-stimulation for IL-2 detection resulted in lower detection of CD25 (compare A and B), and quantification (C) was performed on samples without re-stimulation.

(D and E) Representative plots (D) and frequency (E) of pSTAT5 and CD25 following IL-2 stimulation.

(F and G) Representative plots (F) and frequency (G) of IL-2^+ and IL-2^- out of $CXCR5^+$ gate.

Data are representative of two independent experiments, n = 4 or 5 mice/group. Data are mean ± SEM.

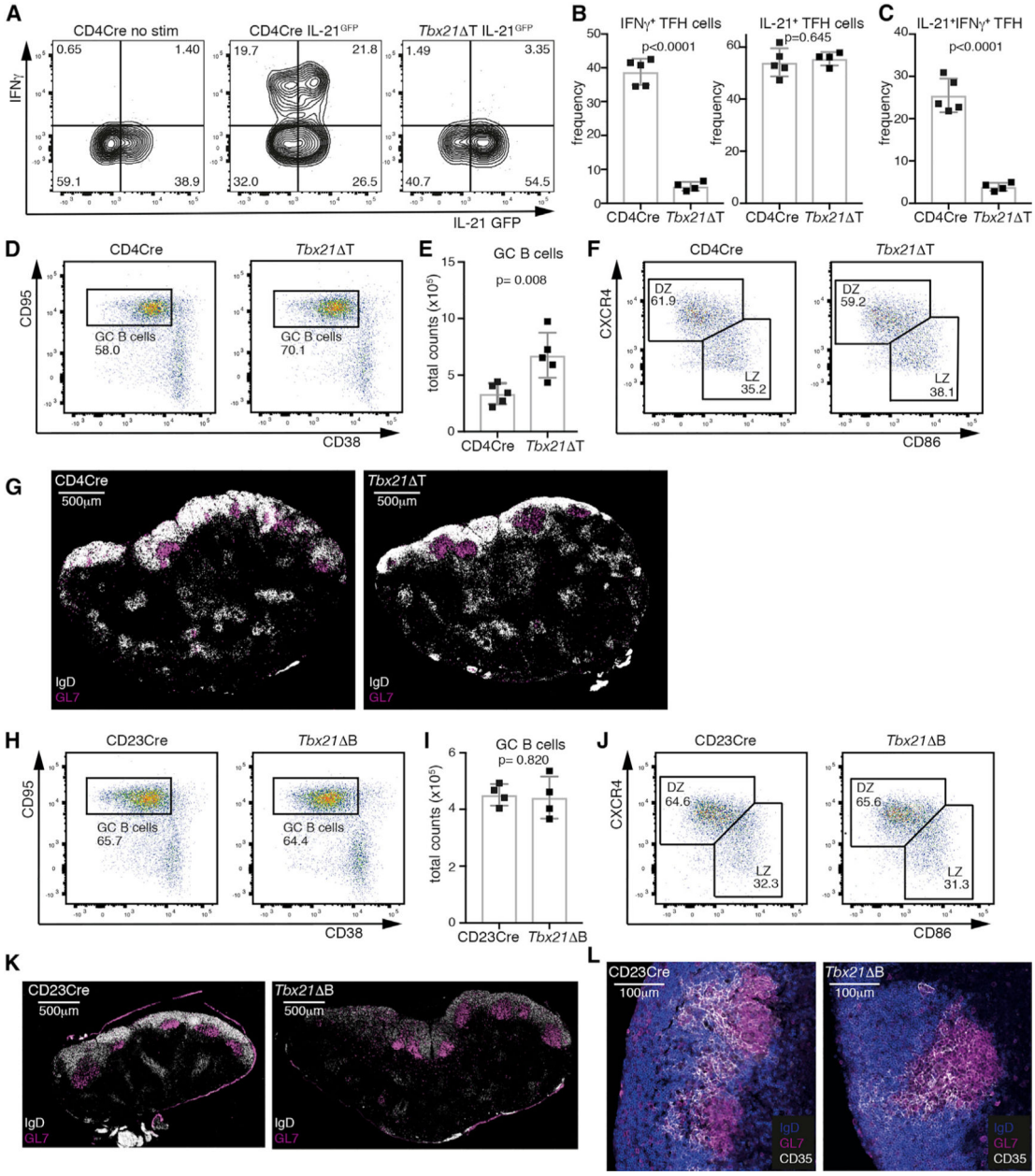

Figure 6. T Cell-Intrinsic T-bet Deficiency Regulates TFH Cytokine Production, While Neither T Cell- or B Cell-Intrinsic T-bet Deficiency Overtly Affects GC Structure

(A–C) CD4Cre_IL-21^{GFP} and *Tbx21*ΔT_IL-21^{GFP} mice were infected with influenza, and dLN TFH (CD44^{+}PSGL-1^{-}Ly6c^{-}PD-1^{+}CXCR5^{+}) cells were re-stimulated and analyzed d8 p.i. Representative flow cytometry plots (A) and frequency (B and C) of IFNγ and IL-21^{GFP} in indicated mice.

(D–G) CD4cre and *Tbx21*ΔT mice were infected with influenza and dLNs analyzed at d8 p.i. Representative flow cytometry plots (D) and total number of GC B cells (B220^{+}IgD^{-}CD95^{+}CD38^{-}) (E). Plots of DZ (CXCR4^{+}CD86^{-}) and LZ (CXCR4^{-}CD86^{+}) GC B cells (F). Confocal micrographs of dLN (white, IgD^{+} B cell follicles; magenta, GL7^{+} GCs) from indicated mice (G).

(H–L) CD23cre and *Tbx21*ΔB mice were infected with influenza, and dLNs were analyzed at d8 p.i. Representative flow cytometry plots (H) and total number of GC B cells ($B220^+IgD^-CD95^+CD38^-$) (I). (J) Plots of DZ ($CXCR4^+CD86^-$) and LZ ($CXCR4^-CD86^+$) GC B cells. Confocal micrographs of dLNs (white, IgD^+ B cell follicles; magenta, $GL7^+$ GCs) from indicated mice (K). Confocal micrographs of dLN GCs from indicated mice (blue, IgD^+ B cell follicles; magenta, $GL7^+$ GCs; white, $CD35^+$ LZ) (L).

In (A)–(F) and (H)–(J), data are representative of three independent experiments, n = 3–5 mice/group. In (G), (K), and (L), data are representative of two independent experiments, n = 3–5 mice/group. Data are mean ± SEM.

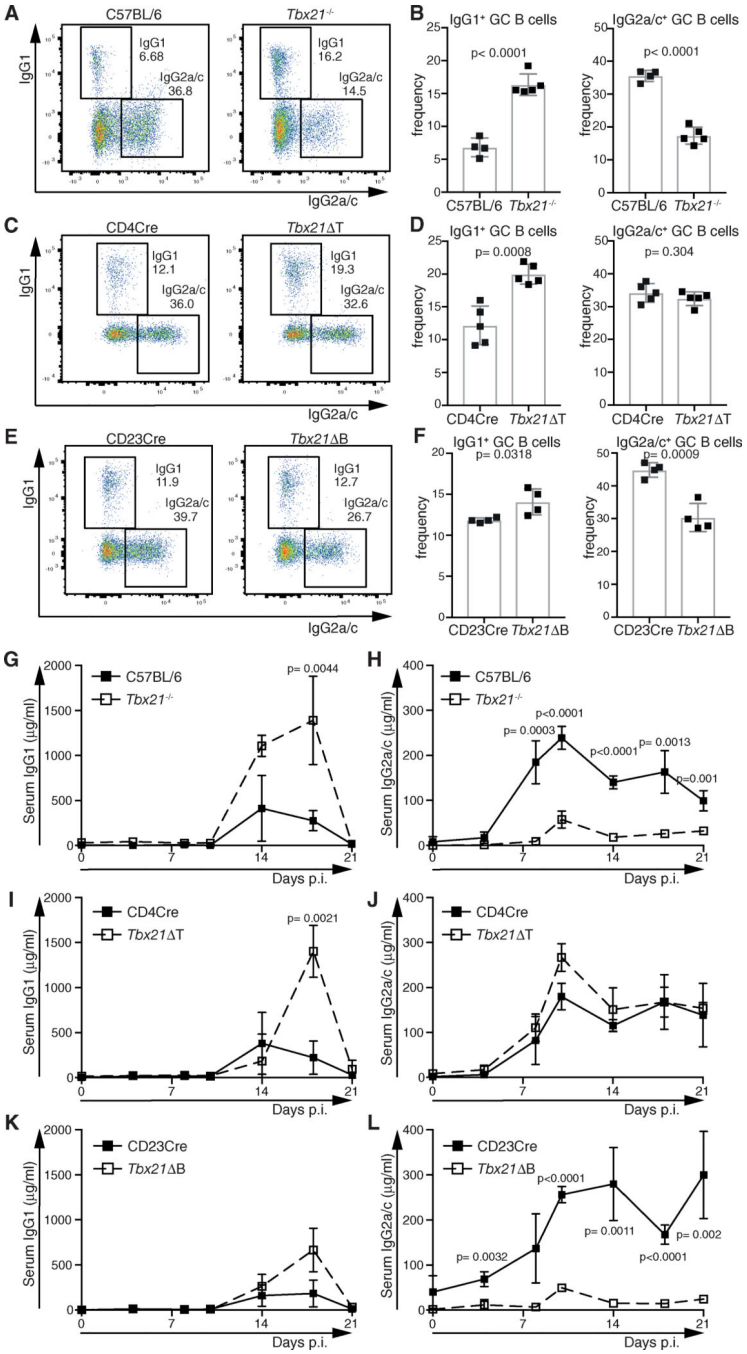

Figure 7. Cell-Intrinsic Role for T-bet in Isotype Class Switching

(A–F) C57BL/6 and *Tbx21*$^{-/-}$ (A and B), CD4Cre and *Tbx21*ΔT (C and D), and CD23Cre and *Tbx21*ΔB (E and F) mice were infected with influenza, and dLNs were analyzed at d8 p.i. (A, C, and E) Representative flow cytometry plots and (B, D, and F) frequency of IgG1 and IgG2a/c surface staining on GC B cells (B220^{+}IgD^{-}CD95^{+}CD38^{-}).

(G–L) C57BL/6 and *Tbx21*$^{-/-}$ (G and H), CD4Cre and *Tbx21*ΔT (I and J), and CD23Cre and *Tbx21*ΔB (K and L) mice were infected with influenza and total serum IgG1 (G, I, and K) and IgG2a/c (H, J, and L) concentrations analyzed at indicated p.i.

In (A)–(F), data are representative of three independent experiments, n = 3–5 mice/group. In (G)–(L), data are representative of two independent experiments, n = 3 or 4 mice/group. Data are mean ± SEM.

KEY RESOURCES TABLE

REAGENT or RESOURCE	SOURCE	IDENTIFIER
Antibodies		
Brilliant Ultraviolet 395-conjugated anti-CD3e (clone 145-2C11)	BD Horizon	Cat#563565; RRID:AB_2738278
Brilliant Ultraviolet 737-conjugated anti-CD4 (clone GK1.5)	BD Horizon	Cat#564298; RRID:AB_2738734
Brilliant Violet 711-conjugated anti-CD162 (clone 2PH1)	BD OptiBuild	Cat#740746; RRID:AB_2740414
APC-Cy7-conjugated anti-CD44 (clone 1M7)	BD PharMingen	Cat#560568; RRID:AB_1727481
Alexa Fluor 488-conjugated anti-Ki-67 (clone B56)	BD PharMingen	Cat#561165; RRID:AB_10611866
Brilliant Violet 711-conjugated anti-CD138 (clone 281-2)	BD Horizon	Cat#563193; RRID:AB_2738060
Brilliant Violet 605-conjugated anti-CD86 (clone GL1)	BD Horizon	Cat#563055; RRID:AB_2737977
Brilliant Violet 510-conjugated anti-B220/CD45R (clone RA3-6B2)	BD Horizon	Cat#563103; RRID:AB_2738007
FITC-conjugated anti-Ig2a/2b (clone R2-40)	BD PharMingen	Cat#553399; RRID:AB_394837
PE-Cy7-conjugated anti-CD95 (clone Jo2)	BD PharMingen	Cat#557653; RRID:AB_396768
Brilliant Ultraviolet 737-conjugated anti-CD127 (clone SB/199)	BD Horizon	Cat#564399; RRID:AB_2738791
Brilliant Ultraviolet 395-conjugated anti-CD8a (clone 53-6.7)	BD Horizon	Cat#563786; RRID:AB_2732919
Brilliant Violet 786-conjugated anti-CD69 (clone H1.2F3)	BD Horizon	Cat#564683; RRID:AB_2738890
Brilliant Violet 786-conjugated anti-CD25 (clone 3C7)	BD Horizon	Cat#564368; RRID:AB_2738771
Brilliant Violet 711-conjugated anti-KLRG1 (clone 2F1)	BD Horizon	Cat#564014; RRID:AB_2738542
PE-Cy7-conjugated anti-IFNγ (clone XMG1.2)	BD PharMingen	Cat#557649; RRID:AB_396766
Brilliant Violet 786-conjugated anti-IgG1 (clone X56)	BD OptiBuild	Cat#742480; RRID:AB_2740814
Brilliant Violet 510-conjugated anti-Ly-6C (clone HK1.4)	Biolegend	Cat#128033; RRID:AB_2562351
PE/Dazzle 594-conjugated anti-CD279 (PD-1) (clone RMP1-30)	Biolegend	Cat#109116; RRID:AB_2566548
Brilliant Violet 421-conjugated anti-CD279 (PD-1) (clone RMP1-30)	Biolegend	Cat#109121; RRID:AB_2687080
Brilliant Violet 421-conjugated anti-CD183 (CXCR3) (clone CXCR3-173)	Biolegend	Cat#126522; RRID:AB_2562205
Brilliant Violet 605-conjugated anti-CD185 (CXCR5) (clone L138D7)	Biolegend	Cat# 145513; RRID:AB_2562208
PerCP-Cy5.5-conjugated anti-CD62L (clone MEL-14)	Biolegend	Cat#104432; RRID:AB_2285839
PE-Cy7-conjugated anti-T-bet (clone 4B10)	eBioscience	Cat#25582582; RRID:AB_11042699
PerCP-Cy5.5-conjugated anti-FOXP3 (clone FJK-16 s)	eBioscience	Cat#45-5773-82; RRID:AB_914351
PerCP-eFluor 710-conjugated anti-CD38 (clone 90)	eBioscience	Cat#46038180; RRID:AB_10852870
PE-conjugated anti-CD184 (CXCR4) (clone 2B11)	eBioscience	Cat#12-9991-81; RRID:AB_891393
PerCP-eFluor 710-conjugated CD122 (clone TM-beta1)	eBioscience	Cat#46-1222-82; RRID:AB_11064442
PE-Cy7-conjugated anti-Phospho-STAT5 (Tyr694) (clone SRBCZX)	eBioscience	Cat#25-9010-41; RRID:AB_2573533
Alexa Fluor 647-conjugated anti-IgD (clone 1126c)	Produced in house	N/A
Alexa Fluor 647-conjugated anti-BCL6 (clone 7D1)	Produced in house	N/A
Alexa Fluor 647-conjugated anti-CD4 (clone GK1.5-7)	Produced in house	N/A
Biotin-conjugated anti-IgD (clone 11-26)	SouthernBiotech	Cat#1120-08; RRID:AB_2631189

REAGENT or RESOURCE	SOURCE	IDENTIFIER
Alexa Fluor 555-conjugated anti-B220 (clone RA3-6B2)	Produced in house	N/A
Alexa Fluor 594-conjugated anti-CD4 (clone GK1.5-7)	Produced in house	N/A
Alexa Fluor 488-conjugated anti-CD4 (clone GK1.5-7)	Produced in house	N/A
Alexa Fluor 647-conjugated anti-GL7 (clone GL7)	Produced in house	N/A
Cy3 conjugated Streptavidin	Jackson Immunoresearch	Cat#016-160-084; RRID:AB_2337244
Dylight 405 conjugated Streptavidin	Jackson Immunoresearch	Cat#016-470-084; RRID:AB_2337248
Brilliant Violet 421-conjugated anti-CD21/CD35 (clone 7G6)	BD Horizon	Cat#562756; RRID:AB_2737772
IgG1-HRP (clone Goat polyclonal)	Southern Biotech	N/A
Unlabeled IgG1 (Goat polyclonal)	Southern Biotech	N/A
IgG1-κ (MOPC31C)	Sigma-Aldrich	N/A
Unlabeled IgG2a (Goat polyclonal)	Southern Biotech	N/A
IgG2c-HRP (Goat polyclonal)	Southern Biotech	N/A
Bacterial and Virus Strains		
Influenza virus strain HKx31 (H3N2)	Produced in house	N/A
LCMV Armstrong	Produced in house	N/A
Biological Samples		
Mouse tissues	N/A	N/A
Chemicals, Peptides, and Recombinant Proteins		
BD Cytofix/Cytoperm	BD	Cat#554714
BioMag Goat Anti-Rat IgG	QIAGEN	Cat#310107
PHORBOL 12-MYRISTATE 13-ACETATE (PMA)	Sigma-Aldrich	Cat#P1585
Ionomycin	Sigma-Aldrich	Cat#I0634
$NP_{311-325}$:1 -A^b-PE (Influenza A $NP_{311-325}$ peptide sequence: QVYSLIRPNENPAHK)	NIH tetramer core	N/A
GP_{66-77}:1-A^b-PE (LCMV GP_{66-77} peptide sequence: DIYKGVYQFKSV)	Moon et al., 2011	N/A
Protein Transport Inhibitor (containing Brefeldin A)	BD	Cat#555029
Protein Transport Inhibitor (containing Monensin)	BD	Cat#554724
FVD eFluor 506	eBioscience	Cat#65-0866
Fixable Viability Stain 700	BD Horizon	Cat#564997
Critical Commercial Assays		
LS columns	Miltenyi Biotec	Cat#130-042-401
Naive $CD4^+$ T Cell Isolation Kit	Miltenyi Biotec	Cat#130-104-453
Brilliant Stain Buffer	BD Horizon	Cat#563794
Foxp3/Transcription Factor Staining Buffer Set	invitrogen	Cat#00-5523
Perm Buffer III	BD Biosciences	Cat# 558050
Lyse/Fix Buffer 5x	BD Biosciences	Cat# 558049
Software and Algorithms		

REAGENT or RESOURCE	SOURCE	IDENTIFIER
Prism	Graph Pad	https://www.graphpad.com/scientific-software/prism/
Flowjo (Treestar)	FlowJo, LLC	https://www.flowjo.com/
Zen Black	ZEISS	https://www.zeiss.com/microscopy/int/products/microscope-software/zen.html
ImageJ	National Institutes of Health (NIH)	https://imagej.nih.gov/ij/index.html
Other		
Superfrost Plus Adhesion Microscope Slides	Thermo Scientific	Cat#J1800AMNT
16% Formaldehyde	Thermo Scientific	Cat#28908
O.C.T Compound	Tissue-Tek	Cat#4583